REPORT DOCUMENTATION PAGE

Form Approved
OMB No. 0704-0188

1. REPORT DATE *(DD-MM-YYYY)*	**2. REPORT TYPE**	**3. DATES COVERED** *(From - To)*
Jan 2014	Technical Paper	Jan 2014- June 2014

4. TITLE AND SUBTITLE

A Method for Eliminating Beam Steering Error for the Modulated Absorption-Emission Thermometry Technique

5a. CONTRACT NUMBER
In-House

5b. GRANT NUMBER

5c. PROGRAM ELEMENT NUMBER

6. AUTHOR(S)

Edward B. Coy

5d. PROJECT NUMBER

5e. TASK NUMBER

5f. WORK UNIT NUMBER
Q0VZ

7. PERFORMING ORGANIZATION NAME(S) AND ADDRESS(ES)

Air Force Research Laboratory (AFMC)
AFRL/RQRC
10 E. Saturn Blvd.
Edwards AFB CA 93524-7680

8. PERFORMING ORGANIZATION REPORT NO.

9. SPONSORING / MONITORING AGENCY NAME(S) AND ADDRESS(ES)

Air Force Research Laboratory (AFMC)
AFRL/RQR
5 Pollux Drive
Edwards AFB CA 93524-7048

10. SPONSOR/MONITOR'S ACRONYM(S)

11. SPONSOR/MONITOR'S REPORT NUMBER(S)
AFRL-RQ-ED-TP-2014-093

12. DISTRIBUTION / AVAILABILITY STATEMENT
Distribution A: Approved for Public Release; Distribution Unlimited

13. SUPPLEMENTARY NOTES
Technical Paper presented at AIAA Aerospace Sciences Meeting, Kissimmee, FL; 5 Jan 2015. PA#14194

14. ABSTRACT

Modulated absorption-emission thermometry (MAET) is a non-intrusive, radiometric technique for measuring line-of-sight average temperature in high-temperature gases. The technique uses alternating measurements of emission and transmission to obtain the emissivity and the radiative intensity of the gas over a spectral band. The temperature is then calculated from the Planck function. The technique does not involve the measurement of spectral features such as line widths or strengths and therefore is suitable for high-pressure environments where spectral lines are broadened and merged. It is also suitable for environments where broadband emitters such as soot are present. Radiometric measurements in general can be made with very high accuracy. The international temperature scale (ITS-90) is realized and disseminated using radiometers and radiance sources for temperatures in the range of 973 K to 4473 K. Radiometry is a primary standard because the governing physical equation (Planck function) does not contain any temperature dependent parameters. Radiometers, or pyrometers, can be purchased off-the-shelf for temperatures from 973 K to 2973 K with accuracies in the range of 2 to 3 K. The technology for creating radiometers is mature, widely available and cost effective. Radiometers for test stand environments can be made that are rugged, compact and require no maintenance. Data acquisition rates in the MHz range and higher are possible using readily available Si, InGaAs and InSb diodes.

15. SUBJECT TERMS

16. SECURITY CLASSIFICATION OF:			**17. LIMITATION OF ABSTRACT**	**18. NUMBER OF PAGES**	**19a. NAME OF RESPONSIBLE PERSON**
					Edward Coy
a. REPORT	**b. ABSTRACT**	**c. THIS PAGE**	SAR	18	**19b. TELEPHONE NO** *(include area code)*
Unclassified	**Unclassified**	**Unclassified**			661-275-5219

Standard Form 298 (Rev. 8-98)
Prescribed by ANSI Std. 239.18

A Method for Eliminating Beam Steering Error for the Modulated Absorption-Emission Thermometry Technique

Edward B. Coy[1]
AFRL/RQRC, Edwards AFB, CA 93524

Nomenclature

I_λ spectral intensity, [W/m^2/Sr/m]

$I_{b\lambda}$ blackbody spectral intensity, Planck function [W/m^2/Sr/m]

s distance in the direction of propagation, m^{-1}

κ_λ absorption coefficient, m^{-1}

σ_λ scattering coefficient, m^{-1}

β_λ extinction coefficient, m^{-1}

$\Phi(s_i, s)$ scattering function, probability intensity propagating in direction s_i will scatter in direction s

λ subscript denotes a spectral quantity

1. Introduction

Modulated absorption-emission thermometry (MAET) is a non-intrusive, radiometric technique for measuring line-of-sight average temperature in high-temperature gases. The technique uses alternating measurements of emission and transmission to obtain the emissivity and the radiative intensity of the gas over a spectral band. The temperature is then calculated from the Planck function. The technique does not involve the measurement of spectral features such as line widths or strengths and therefore is suitable for high-pressure environments where spectral lines are broadened and merged. It is also suitable for environments where broadband emitters such as soot are present.

Radiometric measurements in general can be made with very high accuracy. The international temperature scale (ITS-90) is realized and disseminated using radiometers and radiance sources for temperatures in the range of 973 K to 4473 K. Radiometry is a primary standard because the governing physical equation (Planck function) does not contain any temperature dependent parameters. Radiometers, or pyrometers, can be purchased off-the-shelf for temperatures from 973 K to 2973 K with accuracies in the range of 2 to 3 K. The technology for creating radiometers is mature, widely available and cost effective. Radiometers for test stand environments can be made that are rugged, compact and

[1] Senior Mechanical Engineer, AFRL/RQRC, 10 East Saturn Blvd., Edwards AFB, CA 93524, Senior Member

require no maintenance. Data acquisition rates in the MHz range and higher are possible using readily available Si, InGaAs and InSb diodes.

However, there are many technical challenges involved in relating measurements of radiant intensity to gas temperature. The most basic limitation is that the gas must be in complete thermal equilibrium. If the radiating rotational and vibrational temperatures are different from the translational temperature then radiometric measurements cannot be equated to a thermodynamic temperature using the Planck function. Equilibrium is established through collisions. The collision frequency can be used to estimate the time required for equilibrium to be established. For the conditions of interest in this study, a kinetic theory calculation shows that each molecule will undergo at least 10^{12} collisions per second. If we assume that equilibrium is nearly exact after 10^{3} collisions, local equilibrium will be established in 10^{-9} seconds. Non-equilibrium effects will only be significant for pressures significantly below one atmosphere and low temperatures.

Most substances do not emit thermal radiation in accordance with the Planck function and the emissivity factor must be introduced to relate the actual spectral intensity to that of an ideal Planckian, or black, substance at the same temperature. For the conditions of high pressure combustion systems, the physical basis for the emissivity is the quantum mechanical energy levels of the bound electrons. The energy levels are manifested as spectral lines with distributions and strengths that are in accordance with the Boltzmann distribution. The major products of water and carbon dioxide possess millions of rotational and vibrational lines in the infrared range. Databases of line locations and strengths are available but the net emissivity of the gas, which is the quantity of interest, also depends on the pressure, mole fractions, path-length and temperature. In general the temperature and the mole fractions are unknown so a direct measurement of the emissivity of the gas is usually required, although in some cases the emissivity can be supplied by a fitting to a model. In the case of sooting flames, the emissivity is a result of the nearly black absorption and emission features of soot particles. However, soot concentrations and their optical properties cannot be predicted *a priori* . Based on thermodynamic arguments, for a gas in thermal equilibrium, the emissivity must equal the absorptivity for all wavelengths and directions simultaneously. This principle is known as Kirchhoff's Law. MAET utilizes this principle by making use of absorption measurements to obtain the emissivity and then applying that emissivity to emission measurements to obtain the temperature.

There are a number of technical challenges associated with the absorption measurement. The transmitted light may be scattered or steered away from the detector by index of refraction variations or particles in the flow. If these effects are not compensated for, the emissivity measurement will be erroneously high, and the temperature measurement will be erroneously low. The detector optics must be designed to ensure that the numerical aperture is the same for the measurement conditions and the calibration conditions. If the apertures in the test article limit the solid angle of the rays then the calibration will be invalid. Furthermore, the optics must be designed to ensure that only the region of hot gas that is of interest is within the field of view and cold walls or surfaces which could scatter light are not.

In this report a method for correcting for the effects of beam steering is presented. This report presents the theory of the new technique along with an uncertainty analysis and some results from demonstration experiments.

2. Theory

In this section the relationships between measureable radiometric quantities and the gas temperature are derived. The theory is based on solutions of the radiative transfer equation (RTE) in quasi-steady form[1].

$$\frac{dI_\lambda}{ds} = \kappa_\lambda I_{b\lambda} - \beta_\lambda I_\lambda + \frac{\sigma_\lambda}{4\pi}\int_0^{4\pi} I_\lambda(s_i)\Phi(s_i,s)d\Omega \tag{1}$$

In MAET, the objective is to measure the quantity I_λ at the boundary of the domain and then use the RTE to solve for $I_{b\lambda}$ within the domain. The final step is to use the Planck function to relate $I_{b\lambda}$ to the temperature.

The most basic example of an MAET design is that for a slab of homogeneous, absorbing-emitting, non-scattering gas. In this scenario, shown in Figure 1, three signals are required. The I_0 signal is the source, I_1 is the emission from the gas, and I_2 is the emission plus the fraction of the source that has been transmitted.

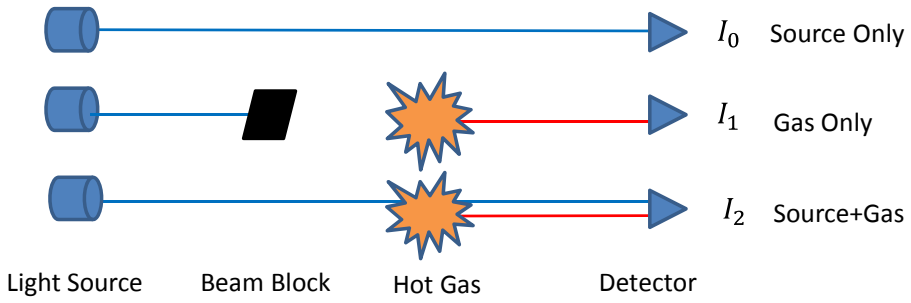

Figure 1 Signals required in a MAET experiment

When light propagates through turbulent gas, beam steering and scattering occur due to fluctuations in density and index of refraction[2,3]. We can correct for these effects if we use two detectors on adjacent spectral bands where the molecular absorption coefficients are different but the scattering coefficients and broadband (soot) absorption coefficients are the same. If the bands are sufficiently close, we can also make the approximation, $I_b \approx I'_b$, where an apostrophe is used to denote a second wavelength. The solutions to the RTE are:

$$I_1 = \frac{\kappa_\lambda}{\kappa_\lambda+\sigma_\lambda} I_b\left(1 - e^{-(\kappa_\lambda+\sigma_\lambda)L}\right) \tag{2}$$

$$I_2 = \frac{\kappa_\lambda}{\kappa_\lambda+\sigma_\lambda} I_b\left(1 - e^{-(\kappa_\lambda+\sigma_\lambda)L}\right) + I_0 e^{-(\kappa_\lambda+\sigma_\lambda)L} \tag{3}$$

The I_1 and I_2 equations can be solved simultaneously for the extinction coefficients, $\beta = \kappa + \sigma$.

$$\beta = \frac{-1}{L} ln\left(\frac{I_2 - I_1}{I_0}\right) \tag{4}$$

Next, the I_1 equations can be solved for the absorption coefficients, κ. Since we are assuming $\sigma=\sigma'$, we have $\beta - \beta' = \kappa - \kappa'$. We arrive at the following expression which relates I_b to measureable quantities.

$$I_b = \frac{1}{\beta - \beta'}\left(\frac{\beta I_1 I_0}{I_0 + I_1 - I_2} - \frac{\beta' I'_1 I'_0}{I'_0 + I'_1 - I'_2}\right) \tag{5}$$

The gas temperature is obtained from the Planck function.

$$T_{gas} = \frac{hc_0}{\lambda k_b ln\left[\frac{2hc_0^2}{I_b \lambda^5} + 1\right]} \tag{6}$$

Estimates of the error can be obtained by propagating the uncertainty in the intensity measurements through equations (4), (5) and (6) using the standard method for combining errors. We assume that the uncertainty is dominated by the random fluctuations in the intensity measurements and that the uncertainties in source signals, I_0, I'_0 and the constants in the Planck function are negligible by comparison. The alternating signals generated by the chopper cause there to be strong correlations in the fluctuations between I_n and I'_n because the sampling is simultaneous, but weak correlations between I_1 and I_2 signals because the sampling alternates slowly relative to the time scales of the flow.

$$\delta T_{gas} = \left(\left(\frac{\partial T_{gas}}{\partial I_1}\delta I_1\right)^2 + \left(\frac{\partial T_{gas}}{\partial I_2}\delta I_2\right)^2 + \left(\frac{\partial T_{gas}}{\partial I'_1}\delta I'_1\right)^2 + \left(\frac{\partial T_{gas}}{\partial I'_2}\delta I'_2\right)^2 + 2\frac{\partial T_{gas}}{\partial I_1}\frac{\partial T_{gas}}{\partial I'_1}\delta(I_1, I'_1) + 2\frac{\partial T_{gas}}{\partial I_2}\frac{\partial T_{gas}}{\partial I'_2}\delta(I_2, I'_2)\right)^{1/2} \tag{7}$$

Where we have introduced the following notation for covariance.

$$\delta(I_n, I'_n) = \frac{1}{N}\sum_{i=1}^{N}(I_n - \overline{I_n})(I'_n - \overline{I'_n}) \tag{8}$$

The estimates for the variances were obtained from the measured data and finite difference approximations of the governing equations were used to obtain the partial derivatives.

3. Prior Work

According to Tourin, the MAET method was originally described by Schmidt in 1909 (Ann. Physik, 29) making it only slightly less venerable than techniques based on Beer's Law which was originally described in 1855. The technique has been referred to in the past as the "Schmidt method" and also the "infrared brightness method", the "Infrared Monochromatic Radiation Method (IMRA)," and the "Planck-Kirchhoff Method." The recent name, "Modulated Absorption-Emission," method is due to Jenkins and Hanson. Early references discuss it as a generalization of the operating principles of the disappearing filament pyrometer, which is an obsolete instrument that was once widely used to measure temperature in furnaces and retorts. It has apparently been independently rediscovered a number of times. Jenkins credited Dyer and Flower. The current author got the idea while modeling radiation heat transfer in a combustion experiment. In any event, there are a number of published works documenting the theory and application of the technique. The more significant ones are summarized in the table. Most of the published applications have been to laminar, sooting, flames at atmospheric pressure, i.e. laboratory experiments. The accuracy of the technique has been validated a number of times with thermocouple measurements under conditions where that was possible. The uncertainty estimates are given in the table.

In each era since its invention, the technique has been updated to exploit new optical technology. One of the main limitations in the past has been the availability of intense light sources that coincide with the strong emission bands. Self's implementation made use of compact quartz-halogen sources. Jenkins's implementation made use of infrared diode lasers and fiber optics. The development of new types of detectors has also been a spur to progress. Tourin describes Silverman's (1949) use of an AC-coupled detector to accomplish the subtraction of the direct flame radiation from the I_2 signal. Self described how silicon photoconductive diodes were more stable and had higher quantum efficiency than photomultiplier tubes. Jenkins developed a theory for a two-color MAET technique that eliminates the need for an absolute intensity measurement and only requires the I_2/I_1 ratio. For pre-mixed, laminar, atmospheric pressure, sooting, flame studies, the simplest theory of MAET should be valid. There is no scattering and the flame zone is homogeneous. The soot increases the emissivity of the flame to a value that is easily measured. Paul developed a theory for the case where scattering, non-absorbing particles were present. Paul's theory accounts for out-scattering and single in-scatter events. Dyer and Flowers applied the technique in a high-pressure combustion bomb with turbulence and presumably scattering, but these issues were not addressed in the theory described in the paper. Tourin described the application of the technique to rocket exhaust plumes but there was no mention of extensions to the basic theory to handle scattering extinction and inhomogeneous flow.

Table 1 Prior work on MAET

Authors	Fuel-Oxidizers	Flame Type	Pressure	Wavelength nanometer	Light Source	Detector	Uncertainty, Comments
Tourin-Krakow, 1965	Propane-O_2/air, pure CO_2 and H_2O	McKenna-type, premixed	1 atm	2400-4900	W-strip lamp	Spectrometer, thermopile	+/- 25K
Tourin, 1966	H2-O2, HC-N_2O_4, IRFNA	Rocket plume, spray flame, industrial burner	1atm	2400-5000	W-strip lamp	InSb, thermopile	+/- 50K
Dyer-Flower, 1981	Propane-air, N_2/O_2/Ar mix	CV bomb Premixed, turbulent	100-1000 psia	Two-color 750, 950	W-strip lamp	Silicon diodes	+/- 25K
Paul-Self, 1989	H_2/CO-O_2	Hencken-type	1 atm	766.5	Quartz-Halogen Lamp	Si diode	+/- 10K Seeded with Potassium
Solomon, Santoro, Semerjian, 1986	Ethylene-air and CO_2, CH_4,C_2H_2, soot, etc.	Coannular diffusion flame, and Heated tube reactor	1 atm	1538-20000	Globar	FT-IR	+/- 50K from 473-1873K
Lyons-Gracia-Salcedo, 1989	Propane-air	McKenna	1 atm	4400	Black-body	NA	"Excellent below 1700K" based on TC
Jenkins-Hanson, 2001	Ethylene-air, Φ=2.1-2.4	McKenna	1 atm	Two-color, 829, 1304	Diode lasers	InGaAs and Si diodes	+/- 20K

4. Experimental setup

The demonstration experiments were carried out using RP-2 fuel and gaseous oxygen at chamber pressures from 25–75 atm and mixture ratios of 2.0-3.4 giving gas temperatures in the range of 3000-3700 K. The injector section of the test article was 5 cm x 5 cm square. This section contracted to 2.5 x 2.5 cm x 22 cm long test section. The optical ports for MAET were located in the center of this section.

The injector produced a uniform mixture ratio with no wall-biasing. The fuel and oxidizer were assumed to be fully mixed and reacted at the measurement location. The average gas velocity at the measurement location was approximately 120 m/s and the Reynolds numbers were in the range of 25,000-100,000.

The windows were designed to allow the MAET optics to be setup quickly and without need for adjustments. The source and detector optics were attached to fixtures that coupled to the windows and held the optics in alignment. The windows that formed the pressure boundary were sapphire and were located approximately 7 cm from the inner wall of the chamber. The windows were angled to prevent an etalon effect. The optical passages in the test article wall were 3 mm holes. Purge gas prevented back flow of combustion gases into the optical passages. The window purge gas had two flow rate settings and was switched during the test using a fast 3-way solenoid valve. The high flow rate was used during startup when the chamber pressure was increasing to ensure no backflow and the low flow was used once chamber pressure stabilized to ensure minimal effect on the measurement. At the low flow rate the momentum flux ratio between the purge flow and the main channel flow was 0.027 or less. The low momentum flux ratio ensured that the jet was deflected by the main channel flow and did not penetrate and disturb the flow that was being measured. The purge gas acted as a window separating the radiating gas from the radiatively inactive purge gas.

The light source was a tungsten halogen lamp. The source was chopped at 500 Hz using a rotating wheel with apertures. The source was coupled to the collimating lens with a multimode fiber optic cable. The pitch optic was an aspheric collimating lens.

The wavelengths selected were 1.3 μm and 1.35 μm. These wavelengths exploit a band head in the near-infrared spectrum of water. A simulation of the emission spectrum of water using the HiTemp database[4] is shown in Figure 2 along with the transmission bands of the filters. The filter bands are also close enough that the differences in the Planck function can be neglected and the value at the average wavelength can be used with negligible error.

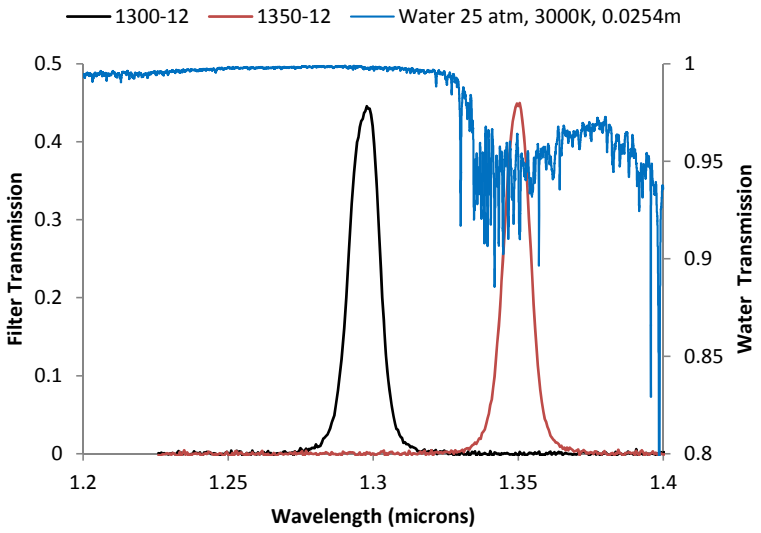

Figure 2 Bandpass filter selection

The sensors were InGaAs diodes. The outputs were amplified 60 dB and low-pass filtered at 5 KHz before digitization. The response was calibrated using cavity blackbody sources over a range of temperatures from 760 to 2530 K with the windows and the 3 mm optical passages in place. It was possible to calibrate with the optical passages because these passages were contained in removable plugs that slid into the wall of the test article and could be removed and connected to the window fixtures.

Two examples of raw signals are shown along with the results of conditional sampling and filtering in Figures 3 and 4. The signals were recorded at 20 KHz with 16 bit resolution. The chopper wheel controller output signal was used to conditionally sample the data and separate it into the two signals, I_1 and I_2. The central 11 points of each window were averaged. This smoothed the data and decimated it to 1 KHz. After decimation an additional 31 point smoothing filter was applied. The first and last 100 samples of the I_2 signal were averaged to obtain the I_0 signal. This step also checked to ensure that window contamination did not occur. In Figure 3, the modulation due to the source was apparent because the gas signal was relatively weak and the absorption of source signal was low. In Figure 4, the gas signal was approximately a factor of 20 higher and the absorption of the source was stronger. The modulation was not as apparent but the algorithm was able to separate the signals.

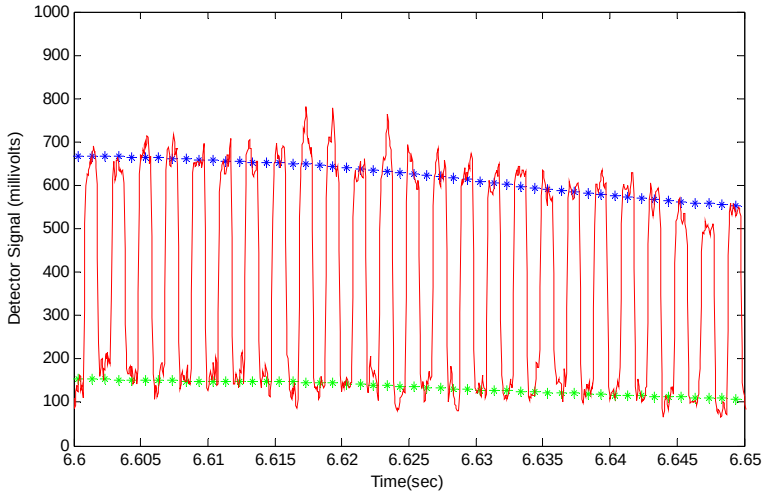

Figure 3 Raw detector signal and conditionally sampled and filtered signals. Low emissivity case.

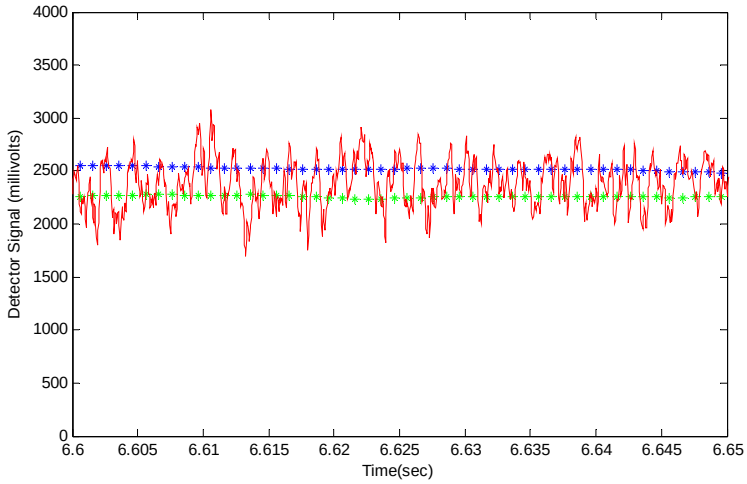

Figure 4 Raw detector signal and conditionally sampled and filtered signals. High emissivity case.

We will now use a typical case to illustrate the application of the technique. The signals and the derived quantities will be related to the events in the operation of the combustion chamber in order to provide a practical understanding of the method. Figure 5 shows the pressure trace from an experiment. The chamber pressure was increased in steps to avoid a hard start (detonation). The dashed vertical lines indicate the portion of the run that is used for obtaining the average values that are reported for temperature, extinction coefficients and so on.

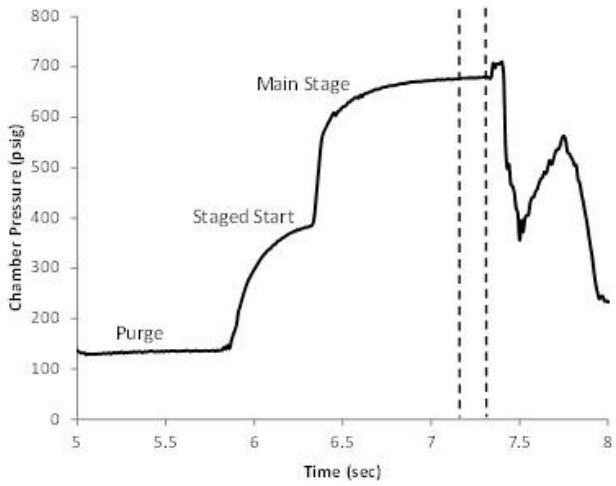

Figure 5 Chamber pressure

Figure 6 shows the detector signals after they have been separated and filtered as described above. The I_1 signals are initially at the noise floor. They rise at 6 seconds during the initial increase of chamber pressure and then increase again at 6.5 seconds as the chamber pressure increases to the target value. The spike in signal at 6.4 seconds may have been caused by a detonation in the chamber which is a common event in the startup of rocket chambers operating with liquid hydrocarbon fuel. This case shows that there is measureable emission from the gas, I_1, at 1.3 μm despite the fact that the value for κ is negligible as shown above in Figure 5. This emission may be due to soot. However, the gas emission at 1.35 μm is much stronger as expected and this difference is the only requirement for the success of the technique. The I_2 signals are initially positive due to the transmission of the source through the non-absorbing (nitrogen) purge gas. The I_2 signals decrease just prior to 6 seconds when the hydrogen-oxygen torch igniter fires and introduces water vapor into the chamber which absorbs the source signal. After 6.5 seconds the I_2 signals increase due to the increased emission from the gas but also perhaps due in part to a decrease in the absorption of the transmitted signal. We would expect that the transmitted signal would be more strongly absorbed at 1.35 μm than at 1.30 μm, but it is not possible to discern that difference in raw signals.

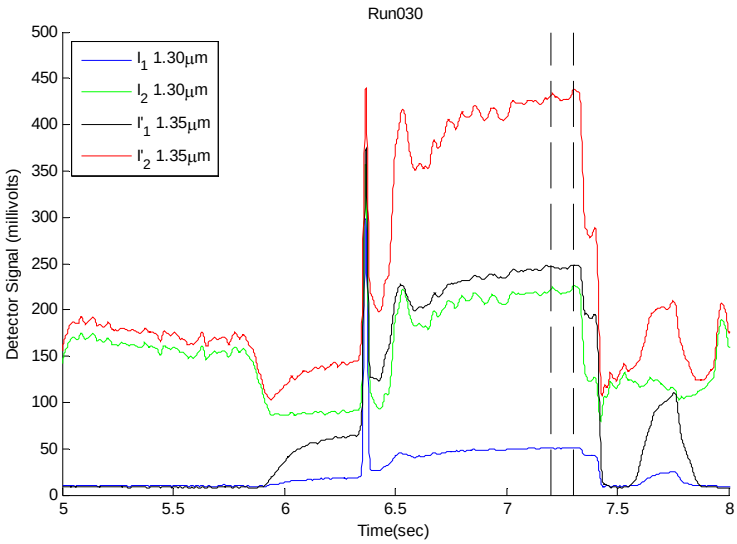

Figure 6 Signals after conditional sampling and smoothing

In Figure 7 the signals have been converted to extinction coefficients, β, using eq. (4). The values of β and β' are identical except during the firing. Note that the MAET technique requires the measurement of $\beta - \beta'$ as shown in eq. (5). When the difference is zero the governing equation (5) is undefined. This occurs a number of times in the interval between 6 and 6.5 seconds. The assumptions of the theory are not valid in this range. The reported measurements are always based on the interval between the vertical dashed lines where the conditions have stabilized. For the case shown in Figure 7, the difference in extinction at the two wavelengths is approximately 1 m^{-1} which is about 5% of the value of the extinction. However, the fact that the value of β and β' are nearly identical except when the chamber is firing supports the assumption that the extinction of the signal due to beam steering is the same at the two wavelengths. The difference in the extinction coefficients is due to the difference in the molecular absorption at the two wavelengths, which is a small fraction of the total extinction, so we see that it is critically important that the theory include scattering effects.

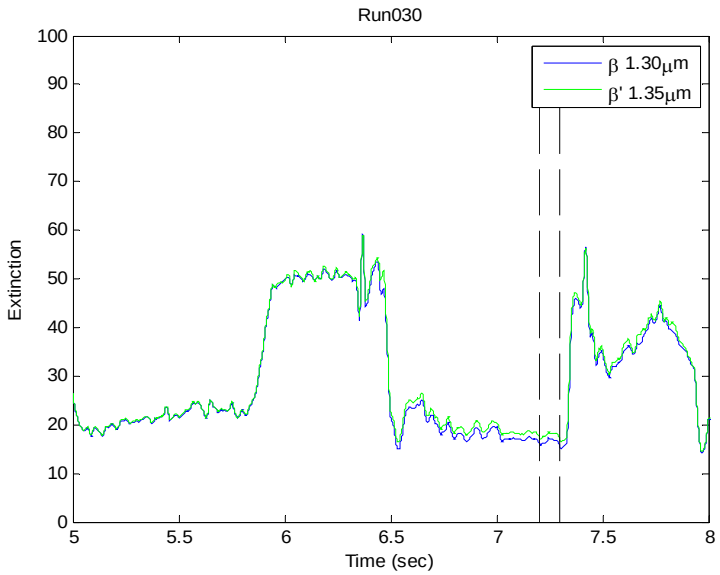

Figure 7 Extinction

Figure 8 shows the final calculation of temperature. The calculated values are shown for the entire time of the test even though the assumptions of the theory are not valid except during the actual firing. The noisy portions of the data would be eliminated if criterion were included to ensure the assumptions were valid.

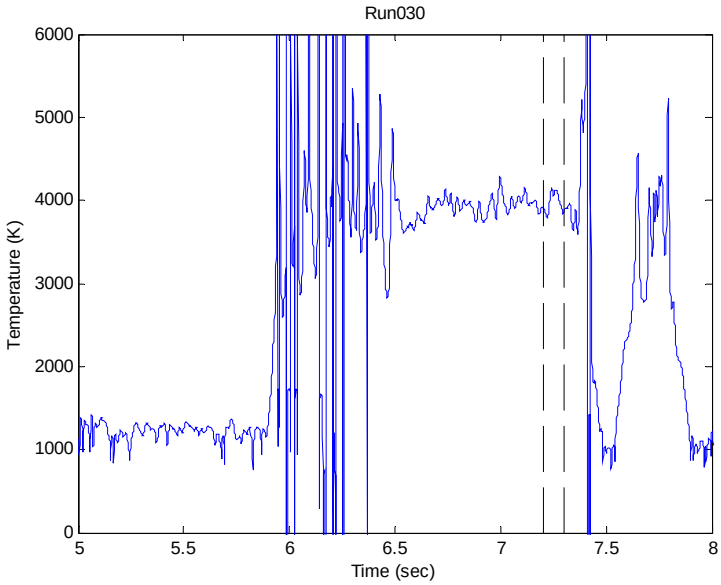

Figure 8 **Temperature**

As an illustration of the significance of the beam steering correction, the data from Run 30 has been reprocessed using the original MAET algorithm. The results are shown in Figure 9. The temperatures are less than half the correct value.

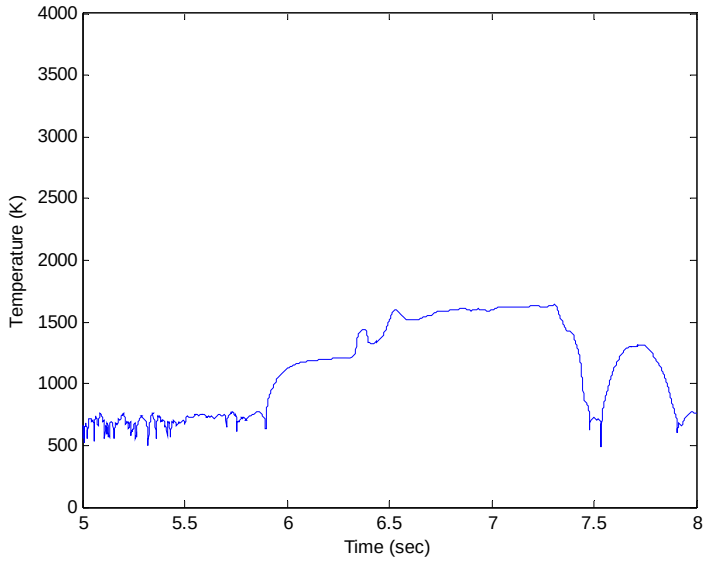

Figure 9 MAET technique with no correction for beam steering. Compare with Fig. 9.

5. Results

The measurement of the extinction coefficient is critical to the success of the technique so it is valuable to examine experimental results for a few more cases to determine if the trends appear reasonable and validate the assumptions. Figure10 shows a case where the bandpass filter was changed from 1.35 to 1.25 μm. The molecular absorption at 1.30 and 1.25 μm is negligible as can be seen by referring to Figure 2. The extinction values shown in Figure 11 are the same for the entire run which supports the conclusion that the scattering and broadband absorption effects that contribute to the extinction are weakly dependent on wavelength. We can expect that the extinction due to scattering and broadband absorption at 1.3 μm is the same as that at 1.35 μm.

Figure 11 shows that the extinction level decreases at reduced pressure, 25 atm, and Figure 12 shows the increase in extinction at 75 atm. Again, the difference in the extinction at the two wavelengths is the critical measurement and it is clear that at high pressures where extinction is strong, the magnitude of the difference is a small fraction of the absolute value and signal to noise ratio is becoming a problem. This shows up clearly in the error estimates given in the data appendix. For the 75 atm case the error estimate is 1900 K which cannot be considered a useful level of accuracy.

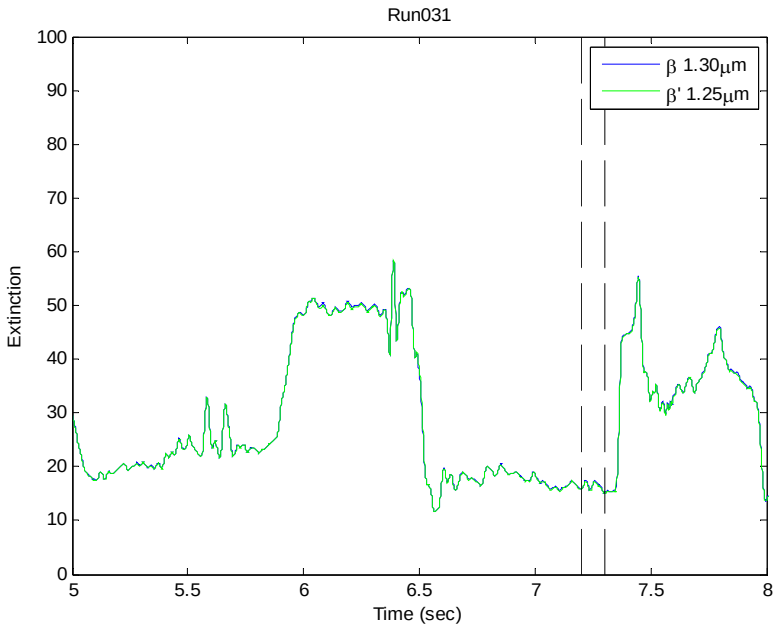

Figure 10 Detector wavelength changed to 1.25 μm

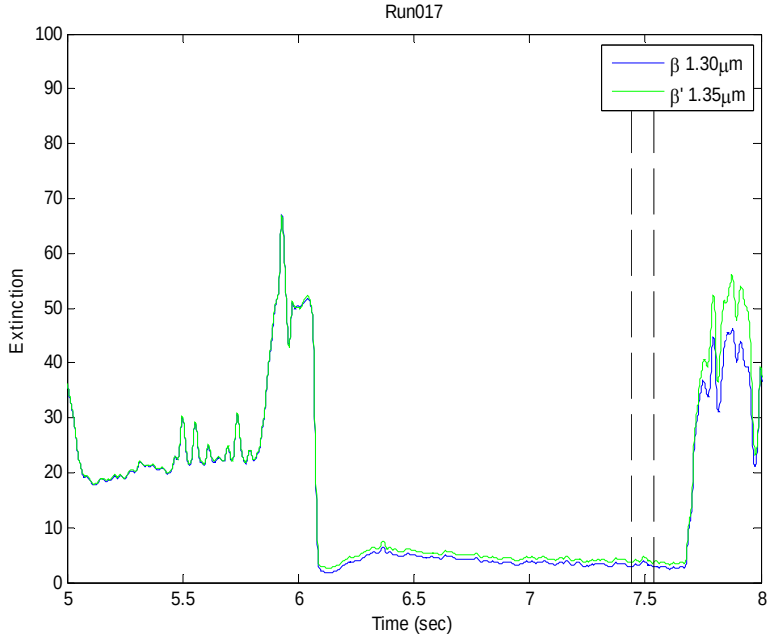

Figure 11 Extinction at 25 atm

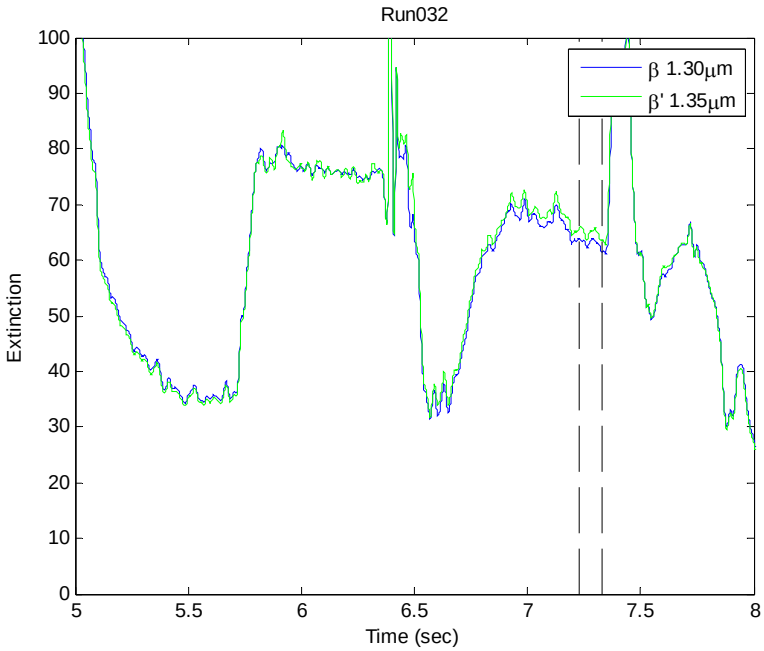

Figure 12 Extinction at 75 atm

The final results for temperature measurement are shown in Figure13. The measurements agree with the equilibrium calculations within 5% which is a useful level of accuracy for boundary layer heat transfer studies in a rocket combustion device.

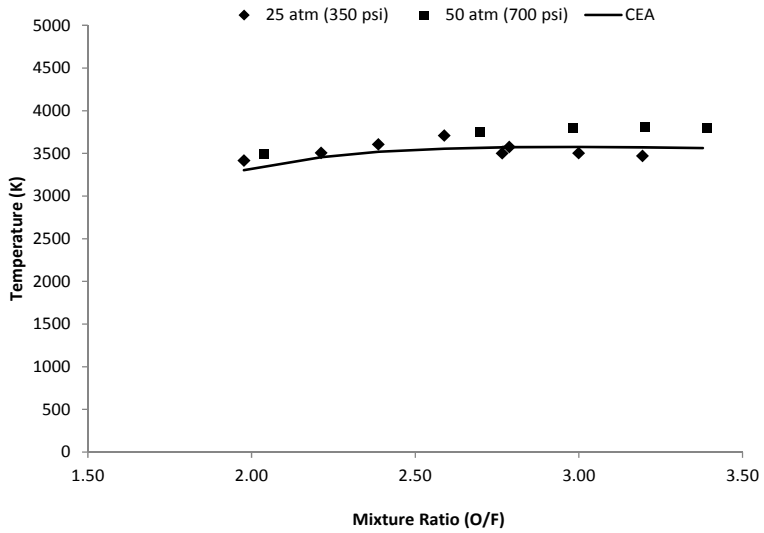

Figure 13 Temperature measurements for all runs

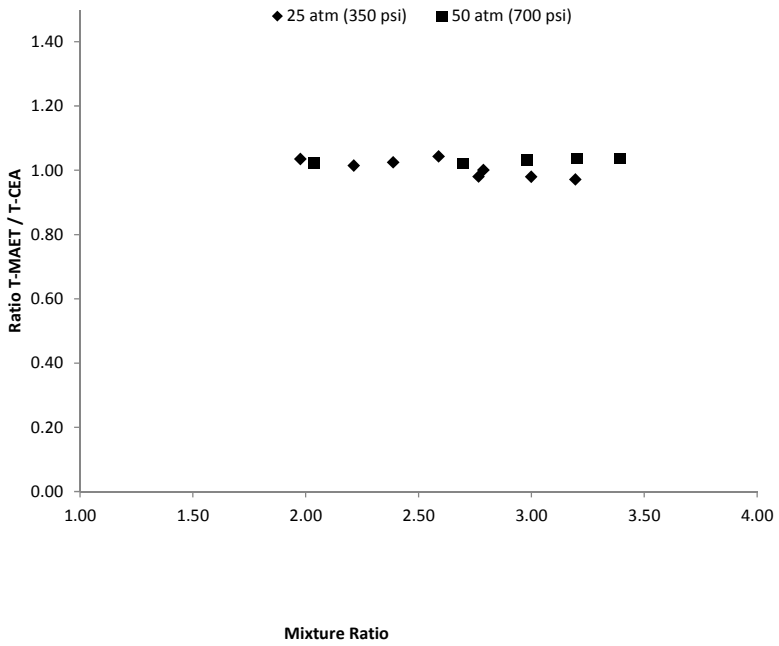

Figure 14 Temperature normalized with adiabatic equilibrium value

The uncertainty of the measurements depends on the details of the run conditions. The estimates are given for each run are given in the data appendix and range from 150 K to 1900 K with the majority falling in the range of 200 K-300 K. There does not appear to be a single component of the signals that dominates the uncertainty. All of the variances and sensitivity coefficients are the same order of magnitude.

6. Conclusions

A method for correcting for beam steering effects in the modulated absorption emission thermometry technique has been demonstrated in a subscale combustion chamber operating with liquid hydrocarbon and oxygen at pressures to 50 atm. Temperatures in the range of 3000-3700 K were measured with an estimated uncertainty of 5%. MAET was shown to be very suitable for the test cell environment. As implemented, it required very little operator involvement and there were no malfunctions. The optical equipment created minimal disruption to the operations or the configuration of the facility. A method for preventing contamination of the test article windows was shown to work successfully.

7. Acknowledgements

The contributions of the following individuals to this work are gratefully acknowledged.

Stephen Danczyk	Test Conductor, Facility Configuration
Earl Thomas	Test Operations, Mechanical Support
Paul Rue	Test Operations, Mechanical Support
Edgar Felix	Test Operations, Procurements
Foster Beasley	Mechanical Design
Ben Gleason	Fabrication
Keith Larsen	Fabrication
Jacob Wood	Summer Student, Optical Modeling

References

[1] Modest, M.F., "Radiative Heat Transfer 3rd ed.," Academic Press, 2013

[2]Fante, R.L., "Electromagnetic Beam Propagation in Turbulent Media," Proceedings of the IEEE, Vol. 63, No. 12, 1975

[3] Kranendonk, L.A., Sanders, S.T., "Optical Design in beam steering environments with emphasis on laser transmission measurements," Applied Optics, Vol. 44, No. 31, 1 Nov. 2005

[4] Rothman, L.S., Gordon, I.E., Barber, R.J., Dothe, H., Gamache, R., Goldman, A., Perevalov, V.I., Tashkun, S.A., Tennyson, J., "HiTemp, the high temperature molecular spectroscopic database," *Journal of Quantitative Spectroscopy and Radiative Transfer*, Vol. 111, No. 15, pp. 2139-2150, 2010

[5] Tourin, R.H., "Spectroscopic Gas Temperature Measurement," Elsevier, New York, 1966

[6]Pfender, E., Spectroscopic temperature determination in high temperature gases, Chapter 6 in "Measurements in Heat Transfer," 2nd ed., edited by Eckert, E.R.G., and Goldstein, R.J., Hemisphere Pub., 1976

[7] Paul, P.H., Self, S.A., "Method for spectroradiometric temperature measurements in two phase flows. 1: Theory," Applied Optics, Vol. 28, No. 11, 1989

[8] Jenkins, T.P., Hanson, R.K., "Soot Pyrometry using Modulated Absorption/Emission," Combustion and Flame 126:1669-1679, 2001